Food and Bioprocess Technology (2025) 18:7484–7501
https://doi.org/10.1007/s11947-025-03903-9

RESEARCH

Fabrication of Electrospun Polycaprolactone Nanofibrous Mats Loaded with Purple Basil Extract (*Ocimum basilicum* L.) as Colorimetric pH Indicator Films

Elif Erez[1] · Ahmet Emin Eroğlu[2] · Beste Bayramoğlu[1]

Received: 30 November 2024 / Accepted: 15 May 2025 / Published online: 28 May 2025
© The Author(s) 2025

Abstract
Intelligent packaging with colorimetric pH indicators revolutionizes traditional food packaging by enabling real-time food quality monitoring. This study used electrospinning to develop pH indicator films from polycaprolactone (PCL) incorporating purple basil extract (PBE). Nanofibrous films containing 0.2% PBE (PCLN_0.2PBE), 0.4% PBE (PCLN_0.4PBE), and 0.6% PBE (PCLN_0.6PBE) were fabricated using different electrospinning conditions. The PCLNs fabricated with a voltage of 20 kV and a flow rate of 1.6 mL/h exhibited the most uniform and bead-free morphology according to scanning electron microscopy. The chemical, thermal, mechanical, and wetting characterization of the films was performed by Fourier transform infrared spectroscopy, differential scanning calorimetry, thermal gravimetric analysis, texture analysis, and contact angle analysis, respectively. Both PCLN_0.4PBE and PCLN_0.6PBE films displayed fast (4–5 s) and clear color transitions ($\Delta E > 3.5$) to successive pH buffers within the range critical for food deterioration, while they exhibited excellent color changes ($\Delta E > 5$) for pH variations of at least two units. The PCLN_0.6 PBE film displayed a ΔE of ~ 5 in only 5 min of exposure to ammonia vapor, whereas PCLN_0.4PBE showed a similar color change for over 15 min. The interaction between the films and acidic and alkaline semi-solid foods was simulated using gelatin gels at pH 2.5 and 11, respectively. Both films displayed significant color transitions ($\Delta E > \sim 9$) within 15 min of contact with the gels, with the response from PCLN_0.6 PBE being more pronounced. The color stability in both films was maintained for up to 14 days at 4 °C, offering potential early warnings against food spoilage. PBE release was evaluated against different food simulants. The highest release occurred in 50% ethanol; the films demonstrated resistance to 3% acetic acid. The findings indicate that electrospun PCL films integrated with PBE have a promising potential to serve as colorimetric pH indicators for monitoring the freshness of food products.

Keywords Nanofiber · Electrospinning · Anthocyanin · Purple basil · Ultrasound-assisted extraction · Freshness indicator

Introduction

The food packaging area, an essential portion of the packaging industry, dynamically creates original solutions to current problems observed by consumer needs and satisfaction. Conventional food packaging no longer meets the needs of most consumers due to issues related to food safety, waste from food and packaging, and shifting lifestyles. As a solution to these challenges, intelligent packaging materials have emerged as a new trend and a popular topic of discussion. Intelligent packaging materials not only protect the food but also monitor the food in real-time, providing information about food quality, which protects the consumers from poisoning cases (Topuz & Uyar, 2020). Intelligent packaging detects and senses changes in internal food conditions during storage and transportation. Colorimetric pH indicator films are a type of intelligent packaging material that respond to pH changes. They display different color changes to inform consumers about these variations. Changes in pH are a vital sign of microbial spoilage and physiological deterioration in food. The generation of significant amounts of volatile basic

✉ Beste Bayramoğlu
bestebayramoglu@iyte.edu.tr

[1] Faculty of Engineering, Food Engineering Department, Izmir Institute of Technology, Gulbahce Campus, Urla, 35430 Izmir, Turkey

[2] Faculty of Science, Department of Chemistry, Izmir Institute of Technology, Gulbahce Campus, Urla, 35430 Izmir, Turkey

nitrogen, such as ammonia, particularly in animal products, leads to shifts in pH levels within the sealed environment (Huang et al., 2024; Li et al., 2024; Shao et al., 2021; Xu et al., 2024). Therefore, colorimetric pH indicators play a crucial role in improving food safety, assessing food quality, and minimizing waste.

Colorimetric pH indicators mainly consist of a color dye sensitive to pH changes and a solid structure supporting the dye (Singh et al., 2018). Synthetic dyes such as bromothymol blue, phenolphthalein, bromocresol green, bromocresol purple, methyl red, atrazine yellow, and alizarin red are used as dye materials (Agarwal et al., 2012; Schoolaert et al., 2016; Van der Schueren et al., 2010). However, these synthetic dyes might migrate to the food and create toxic and carcinogenic issues, which can cause severe conditions to human wellness besides the negative environment effects (Yildiz et al., 2021). Therefore, the preference for natural color pigments over synthetic dye has been accelerated in recent years. As natural color pigments, anthocyanins are non-toxic, safe, and water-soluble and show distinctive colors at different pH values because of their unstable nature to pH. Phippen and Simon (1998) showed that purple basil is an abundant source of acylated and glycosylated anthocyanins compared to other anthocyanin sources, providing a unique source of stable color pigments for the food industry. A previous study in our group demonstrated that purple basil extract (PBE) is a potential alternative to synthetic pH-indicator dyes owing to its abundance in anthocyanins (Erez & Bayramoglu, 2024).The extraction of anthocyanins and phenolic compounds from dried purple basil leaves was carried out by ultrasound-assisted extraction (UAE), and the process parameters were optimized to maximize the total monomeric anthocyanin (TMA) content and the increase in green intensity (IGI) with pH change. The latter response was considered a measure of the colorimetric pH-indicator ability of the extracts. The outcomes highlight the potential use of PBE as a pH-indicator and antioxidant material as well as a colorant in the food industry. This study is a follow-up investigation into developing potential intelligent pH indicator films integrated with PBE.

Encapsulation is the entrapment of a bioactive compound into the polymer matrix to protect and deliver a bioactive compound to a targeted site. The sensing ability of colorimetric pH indicators can be improved by increasing the specific surface area of the reacting molecule. Electrospinning has recently attracted attention as a promising nanotechnology-based nanofiber fabrication technique to encapsulate bioactive compounds with a high efficiency. The fundamental principle of this method relies on exposing a polymer solution to electrical forces, which results in elongated ultrathin fibers produced at submicron to the nanoscale with high surface-to-volume ratio and porosity, good mechanical properties, and controllable morphology (Mercante et al., 2017; Wongsasulak et al., 2010). The characteristic high surface-to-volume ratio of the nanofibers provides benefits for an efficient intelligent indicator system such as high encapsulation efficiency and rapid responsiveness to changes in the surrounding medium, enabling fast detection of food quality changes. Moreover, the non-thermal nature of the electrospinning process makes it a desirable approach to encapsulate heat sensitive bioactive compounds like anthocyanins (Forghani et al., 2021). In this work, PCL was chosen as the base polymer to encapsulate PBE into nanofibers through electrospinning. PCL is a hydrophobic aliphatic linear, semicrystalline, thermoplastic polyester, primarily used in biomedical and tissue engineering applications. It has gained increasing interest for food packaging applications because it is a Food and Drug Administration (FDA)-approved polymer (Dumitriu et al., 2021). Moreover, PCL's semi crystalline structure and hydrophobic nature slow the degradation rate depending on the molecular weight and enable good mechanical properties in polymeric films (Azari et al., 2021; Cipitria et al., 2011). PCL has commonly been used in the development of electrospun pH indicator colorimetric films incorporating synthetic or natural dyes by many scholars in the literature (Guclu et al., 2023; Jovanska et al., 2022; Liu et al., 2022; Luiza et al., 2021; Oliveira Filho et al., 2024; Silva et al., 2019; Zou et al., 2024).

Despite the high anthocyanin content of purple basil extract, only a few studies have recently explored its use in the fabrication of pH sensitive indicator films so far. Ebrahimi et al. (2022) developed intelligent films by solvent-casting a mixture of gelatin and purple basil leaf extract to monitor the freshness of chicken fillets. Barkhordari et al. (2024) casted a multifunctional pH-responsive nanocomposite film from gelatin, TiO_2, and PBE and monitored fish freshness. Both studies demonstrated the potential of PBE as a natural pH indicator dye to incorporate into intelligent packaging materials. However, the use of hydrophilic biopolymers like gelatin limits the application of the developed material due to high water solubility and swelling. While hydrophilicity in films is beneficial for enhancing the reaction sensitivity of the indicator dye, it may compromise the structural integrity of the film. Conversely, utilizing hydrophobic polymers to maintain the film's self-integrity could lead to reduced reaction sensitivity of the dye (Zhang et al., 2022). To address this contradiction, new methods such as electrospinning are necessary for creating nanofibrous films made from hydrophobic polymers. These films possess a high surface area-to-volume ratio, which allows for an enhanced interaction between the encapsulated pH indicator dye and the surrounding medium. To our knowledge, there are currently no published reports on the utilization of PBE into electrospun nanofibrous films. This study represents the first effort to use PBE in the fabrication of colorimetric pH indicator nanofibrous films using the electrospinning technique.

The effects of electrospinning parameters and PBE content on the morphological properties of the nanofibrous films were investigated. The films exhibiting the most uniform and bead-free nanofibers were characterized further in terms of their color response to pH change and volatile ammonia, color stability, mechanical, wetting, and thermal properties, functional group identification, and release behavior in different types of food simulants.

Materials and Methods

Materials

Purple basil (*Ocimum basilicum* L.), grown in the Arapgir region of Malatya (Turkiye), was purchased in dried form from Arapgir Municipality (August 2019) and stored in a refrigerator (4 °C) until use. Acetic acid (glacial), sodium acetate, sodium carbonate, and sodium chloride were purchased from Merck (Darmstadt, Germany). Glycine, potassium chloride, potassium phosphate monobasic, potassium phosphate dibasic, sodium hydroxide, sodium phosphate dibasic, and polycaprolactone (Mn 80,000) were purchased from Sigma-Aldrich (St. Louis, MO, USA). Ethanol (99.9%) (Isolab, Wertheim, Germany), chloroform (Isolab), N,N-Dimethylformamid (Isolab), and sodium phosphate monobasic (Riedelde Haën, Seelze, Germany) were purchased from companies mentioned in parentheses.

Extraction of Dried Purple Basil Leaves

UAE was used to obtain PBE from dried purple basil at optimized conditions (55.25% ethanol containing 0.1% acetic acid, 30 mL/g solvent/solid ratio, 39.24 min) at 35 ± 3 °C according to the method developed previously in our group. The optimized conditions were determined based on the combined response of maximum total monomeric anthocyanin (TMA) content and the pH-dependent increase in green intensity (IGI). The interested reader should refer to Erez and Bayramoglu (2024). The extracts were filtered using 0.45 µm cellulose-acetate filters (Chromafil CA-45/25, Germany). The solvent in the extract was evaporated in a rotary evaporator (Heidolph Laborota-4000, Germany) under vacuum. The fresh extracts were lyophilized (Labconco, USA) and stored at 4 °C until use.

Preparation of Electrospinning Polymer Solutions

10% (w/v) PCL control solution (without the extract) was prepared in 1:1 (v/v) DMF:chloroform. The mixture was stirred overnight using a magnetic stirrer (Ika-Werke, Germany) to obtain a homogenous solution. To prepare the electrospinning solutions incorporating the extract, the lyophilized PBE was first dissolved in DMF until no particulate matter was visible. Later, chloroform was added such that the DMF/chloroform (v/v) ratio was 1:1. The required amount of PCL was added to the mixture to prepare a 10% PCL solution (w/v), and the mixture was stirred overnight. Three different PBE concentrations (0.2%, 0.4%, and 0.6% w/v) were studied to investigate the effect of PBE content on the nanofibrous membrane properties.

Rheological Behavior of Polymer Solutions

The polymer solutions' rheological properties were measured using a controlled AR 2000ex Rheometer (TA Instruments, USA) with a 20 mm parallel plate geometry (gap width = 1000 µm). The temperature was set to 25 ± 1 °C. The shear rate varied from 1 to 100 s^{-1}. The shear stress (τ) versus shear rate (γ) data were collected and fitted to the power-law model (Eq. 1). Measurements were done in triplicate.

$$\tau = k(\gamma)^n \tag{1}$$

Here, τ is the shear stress (Pa), γ is the shear rate (s^{-1}), k is the consistency coefficient ($Pa.s^n$), and n is the flow behavior index.

Electrospinning Process

Electrospun nanofiber mats were fabricated using the Nanospinner basic system (Inovenso, Turkiye) via a procedure schematically presented in Fig. 1. PCL solutions with or without PBE were placed in a 20 mL syringe with a 21 mm inner diameter fitted with a 0.2 mm inner diameter metallic needle. The syringe was horizontally placed. The square-shaped stationary collector was covered with aluminum foil.

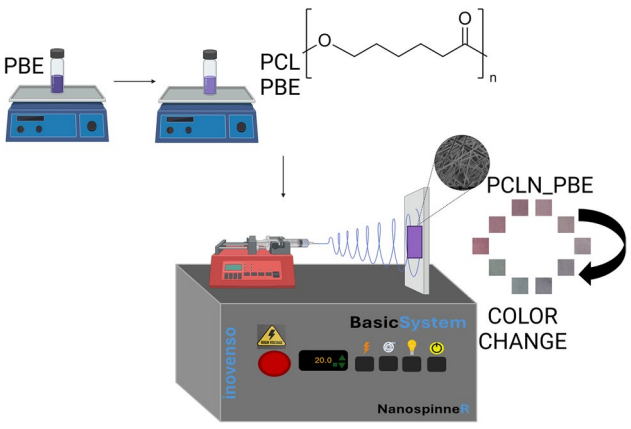


Fig. 1 Schematic illustration of the electrospinning procedure and fabrication of PCLN_PBEs. Created in BioRender. EREZ, E. (2024) https://BioRender.com/c42q933

The electrode was connected to the collector. The distance between the tip of the syringe and the collector was 26 cm. The flow rate was adjusted with a syringe pump (NE-300, USA). 10% (w/v) PCL solutions with different PBE concentrations (0%, 0.2%, 0.4%, 0.6% w/v) were electrospun and labeled as PCLN, PCLN_0.2PBE, PCLN_0.4PBE, and PCLN_0.6PBE, respectively. Electrospun films were fabricated with a 20 kV or 25 kV voltage and a flow rate of 1.6 mL/h or 2.0 mL/h in 3.5 h. These process parameters were determined by preliminary experiments using pure PCL solutions. The films were maintained at room temperature inside plastic bags in dark before any analyses.

Morphology of the Nanofibrous Mats

The morphological properties of nanofibers were determined using SEM (FEI Quanta 250 FEG, USA) with a voltage of 3 kV, 2.5 cm of spot, and an ETD detector. Nanofibrous films were cut into fragments and coated with a thin gold layer for 30 s via a sputter coater (Emitech K550X). Then, they were stuck on metal stubs, and the surface images were taken. Micrographs were taken at different magnifications for the surface, but ×5000 magnification was used for comparisons. The diameters of randomly selected 60 fibers were measured and analyzed using ImageJ software.

Film Thickness

The film thickness was measured with a digital micrometer (Chronos, UK) from five randomly chosen locations on a single film.

Fourier Transform Infrared (FT-IR) Spectroscopy

FT-IR spectrophotometer (UATR-2 Perkin Elmer, UK) was used to analyze the characteristic intramolecular chemical bonds in PBE powder and PCLNs with different PBE concentrations. Scans were performed in the 400–4000 cm^{-1} at 0.4 cm^{-1} resolution.

Thermal Analysis of Electrospun Nanofibrous Mats

Differential scanning calorimetry (DSC) (DSC 6000, Perkin Elmer, USA) and thermal gravimetric analysis (TGA) with a simultaneous thermal analyzer (STA 8000, Perkin Elmer, USA) were used for the thermal analysis of the PCLNs. The methods by Hu et al. (2024), Shi et al. (2022), and Zou et al. (2023) were used with slight modifications. For DSC analysis, 5–10 mg of the films were enclosed in a hermetically sealed aluminum pan, and the samples were heated from 10 to 200 °C at a rate of 10 °C min^{-1}. For TGA analysis, 5 mg film was enclosed in a hermetically sealed aluminum pan, and the samples were heated from 25 to 600 °C at a rate of 10 °C min^{-1}. Both systems were purged with nitrogen gas at a flow rate of 50 mL min^{-1}.

Mechanical Properties of the Films

The tensile strength (TS), elongation at break (EB), and Young modulus (YM) of electrospun films were determined using a texture analyzer TA-XT2 (Stable Microsystems, Godalming, UK) following the ASTM Standard Method D882-02 (ASTM, 2002) guidelines. Film strips measuring 80 mm × 10 mm were secured at an initial grip distance of 50 mm. The test speed was set at 50 mm/min, and a load of 5 kg was applied. Each sample was tested with eight replicates.

Contact Angle Measurements

The hydrophilicity of the films was assessed using contact angle analysis with an Attension Theta Tensiometer (Biolin Scientific, Sweden). Five microliter of distilled water was placed on the film surface, and the measurement was taken around the drop. The measurements were made in triplicate.

Color Change Response of Electrospun Films to Various pH Buffers, Ammonia Vapor, and Gelatin Gels at Different pH Values Simulating Semi-solid Foods

Electrospun films were cut into squares (1.5 cm × 1.5 cm) and immersed in 2 mL buffer solutions with pH values ranging from 1 to 10 to evaluate the nanofibers' pH sensitivity. PCLN_0.2PBEs were treated for 5 min, whereas PCLN_0.4PBEs and PCLN_0.6PBEs were treated for only 5 s to observe a perceptible color change. Afterward, the color parameters (L^*, a^*, b^*) were measured by a colorimeter (CR 400 Konica Minolta, Japan). The measured L^*, a^*, and b^* values were used to calculate the change in color (ΔE) with pH values according to Eq. 2,

$$\Delta E = \left[\left(\Delta L^*\right)^2 + \left(\Delta a^*\right)^2 + \left(\Delta b^*\right)^2\right]^{0.5} \quad (2)$$

where $\Delta L^* = L - L_{0^*}$, $\Delta a^* = a - a_{0^*}$, and $\Delta b^* = b - b_{0^*}$. L_0^*, a_0^*, and b_0^* are the initial color parameter values of the corresponding film at a certain pH. More specifically, ΔE of pH 4 is calculated using the color parameters of pH 3 as a reference, while ΔE of pH 5 is calculated using the color parameters of pH 4 as a reference. On the other hand, ΔE response of the films at pH 5 in going from pH 3 to 5 is calculated with the color parameters of the film at pH 3 taken as a reference. This type of calculation guarantees perceptible changes from one pH to another. The only exception is the ΔE for pH 1, which was calculated using the nanofibers not

yet in contact with any buffer solution as reference (Silva et al., 2019). Others have also used this approach to calculate ΔE values (Moreira et al., 2018; Prietto et al., 2018). The control film, PCLN, was also treated the same way as PCLN_0.2PBE, PCLN_0.4PBE, and PCLN_0.6PBE. Photographs of the films were taken by Samsung Galaxy A21 smartphone (Korean) in pro mode (ISO = 800 and WB = 10,000 K) under the same lighting conditions. Photoshop, version 6.0 (Adobe Systems Inc., San Jose, CA, USA) was used to crop the images for publication.

The pH indicator ability of electrospun nanofiber mats was also evaluated in terms of their color change response to ammonia vapor, following the method of Duan et al. (2023) and Goudarzi et al. (2023) with slight modifications. The films were cut into square pieces (2 cm × 2 cm) and fixed on the cover of glass petri dishes with the help of a double-sided tape. The interaction of the films with ammonia vapor started after the cover was placed on the petri dish containing 30 mL of 0.8 M ammonia solution. The color parameters were recorded every 5 min by a colorimeter (CR 400 Konica Minolta, Japan) for 30 min. The color change (ΔE) of the films was calculated via Eq. 2, taking the initial ($t = 0$ min) color parameters as the reference values.

Lastly, the pH indicator capabilities of the films were evaluated in terms of their color change response to gelatin gels (prepared from 30 mL of 7.5% w/v aqueous solutions) at pH 2.5 and pH 11, which simulate, respectively, the acidic and alkaline semi-solid foods. This analysis followed the methodology described by Musso et al. (2017). The films were cut into square pieces (2 cm × 2 cm) and placed on the gelatin gels within petri dishes. The color parameters were recorded every 15 min using a colorimeter (CR 400 Konica Minolta, Japan) for a total duration of 30 min. The color change (ΔE) of the films was calculated via Eq. 2, with the initial color parameters at $t = 0$ min used as reference values.

Color Stability of the Films

PCLN, PCLN_0.4PBE, and PCLN_0.6PBE were cut into squares (1.5 cm × 1.5 cm) and stored in desiccators with 75% relative humidity in incubators (Zicheng (ZDP-A2120), China; Sanyo Incubator-MIR-153, Japan) at 25 °C and 4 °C for 28 days to evaluate the color stability of the pH indicator electrospun films. The methods by He et al. (2023), Li et al. (2022), Zhang et al. (2022) were used with slight modifications. During storage, the color parameters (L^*, a^*, b^*) were measured by a colorimeter (CR 400 Konica Minolta, Japan) twice a week. The measured L^*, a^*, and b^* values were used to calculate the color change (ΔE) according to Eq. 2, where the reference values were taken as the initial color parameters of the films.

In Vitro Food Simulant Release Assays

The extract release rate from the pH indicator nanofibrous films to different food simulants was determined according to the method by Alizadeh-Sani et al. (2021) with some modifications. Firstly, PCLN_0.4PBE and PCLN_0.6PBE were cut into squares (2 cm × 2 cm) and weighed (Shimadzu AUW-220D, Japan). The release rate from the films was tested in three different food simulants, i.e., distilled water, 3% acetic acid, and 50% ethanol, representing hydrophilic foods with a pH above 4.5, acidic aqueous, and lipophilic foods, respectively (Commission Regulation (EU) No 10/2011). The films were immersed in 20 mL of the corresponding solutions, and the system was gently shaken at constant 100 rpm in an incubator (Sartorius Shaker Certomat BS-1, Germany) maintained at 25 °C or 4 °C for 6 h. Samples were taken at time intervals of 30 min, and the absorbance values (at 525 nm) were recorded over time using a UV–vis spectrophotometer (Shimadzu, UV-2450, Japan). After each measurement, the sample in the cuvette was poured back into the original flask to maintain the total volume constant. The release rate in each food simulant was expressed in terms of mg PBE/mg film using a calibration curve. The experiments were performed in triplicates.

Statistical Analysis

Minitab version 18 (Minitab Inc., PA, USA) was used for experimental design, regression, and statistical analyses. Data were presented as mean ± SD after at least three independent runs. Significant differences between the experimental data were analyzed using Tukey's pairwise comparison test ($P < 0.05$).

Results and Discussion

Variation of Electrospinning Solution Viscosity with PBE Concentration

The viscosity of the polymer solution, which is influenced by both the concentration of the polymer and the type of solvent, is a critical factor in creating a stable jet of polymer solution to ensure spinnability. If the viscosity is too low, the polymer solution fails to entangle properly, forming beads or droplets (Mercante et al., 2017). Conversely, excessively high viscosity can impede the flow of the polymer solution through the needle tip, thus preventing fiber formation (Aman Mohammadi et al., 2020).

The rheological properties of the electrospinning solutions with varying concentrations of PBE were determined to aid in understanding the morphological differences in the fabricated nanofiber mats. The flow behavior of the solutions

was well-explained by the "Power Law Model" ($R^2 \sim 0.99$). Table S1 summarizes the resulting fitting parameters, and Fig. S1 shows the variation of solutions' apparent viscosity with the shear rate. The flow behavior index, *n*, was lower than 1 for all the samples, indicating shear-thinning behavior. The apparent viscosity of the solutions increased with PBE concentration (from 0.299 ± 0.082 Pa.s for neat PCL to 0.494 ± 0.029 Pa.s for PCL with 0.6% PBE, at 50 s^{-1} shear rate). These findings are in alignment with the literature. Prietto et al. (2018) reported that the viscosity of zein solutions significantly increased with the incorporation of red cabbage anthocyanins. Luiza et al. (2021) observed that the apparent viscosities of the PCL/PEO solutions increased with the addition of phycocyanin and curcumin. In a study by Moreira et al. (2019), it was shown that the phycocyanin addition promoted an increase in the solution viscosity.

Morphological Characteristics

The surface morphology of the electrospun nanofibrous films was examined using SEM to analyze the impact of process conditions and PBE concentration. Table 1 presents the fiber diameter measurement results for all films. The control films (10% w/v PCL, no PBE) were electrospun under four electrospinning conditions and denoted as PCLNs. The corresponding SEM images are presented in Fig. S2, showing that the electrospinning conditions significantly influenced the fiber morphology. Bead formation was observed in all four films; however, spherical beads transformed into elongated ones with lower flow rate. The mats electrospun at a 20 kV voltage and a flow rate of 1.6 mL/h exhibited the least number of beads (elongated in shape) and relatively more uniform morphology compared to the others. Moreover, the fiber diameter increased with higher voltage, while the opposite trend was observed with increased flow rate. These findings are consistent with Haider et al. (2018), who noted that an increase in applied voltage could result in the formation of beaded nanofibers, associated with a decrease in the size of the Taylor cone and an increase in the jet velocity at the same flow rate. They also mentioned that higher voltages might lead to an increase in fiber diameter due to the increased jet length (Haider et al., 2018).

Figures S3, S4, and S5, respectively, show the surface morphologies of the films labeled as PCLN_0.2PBE, PCLN_0.4PBE, and PCLN_0.6PBE, electrospun at four processing conditions. Speaking of PCLN_0.2PBE films, fewer and smaller beads were observed in those processed at a flow rate of 2 mL/h compared to their counterparts electrospun from plain PCL solutions (PCLNs), whereas there were no beads in films electrospun with a flow rate of 1.6 mL/h. The electrospinning conditions influenced the presence of beads within the nanofibers (Fig. S3) but did not statistically impact the fiber diameter. This observation was also valid for PCLN_0.4PBE films (Fig. S4). The films spun at a 20 kV voltage and a flow rate of 1.6 mL/h exhibited the most uniform nanofibers among those spun at other conditions. The disappearance of beads with a decreasing flow rate can be attributed to more complete solvent evaporation during the polymer jet's flight from the needle tip to the collector (Haider et al., 2018). Finally, PCLN_0.6PBE films electrospun with a voltage of 20 kV had more uniform and bead-free morphology (Fig. S5). Similar to control PCLNs, the process conditions significantly affected the fiber diameter. Films spun at a voltage of 20 kV and a flow rate of 1.6 mL/h, and films spun at 25 kV and 2 mL/h exhibited smaller fiber diameters than the others. Overall, considering all the electrospinning process conditions, the most bead-free and uniform nanofibers were obtained with a voltage of 20 kV and a flow rate of 1.6 mL/h. Hence, only the films fabricated using these parameters were subjected to further tests. The corresponding SEM images and the fiber diameter distributions for PCLNs having different PBE contents are given in Fig. 2. It is also important to note that PCLN_0.2PBE films were excluded from further characterization methods due to their inadequate performance as pH indicators (see "Colorimetric pH-Indicator Performance of the Nanofibrous Films" section).

The effect of PBE concentration on nanofiber diameter and morphology correlated with its effect on solution viscosity. The incorporation of PBE into the electrospinning solution increased its apparent viscosity, as shown in the "Variation of Electrospinning Solution Viscosity with PBE Concentration" section, and improved the fiber morphology. Under certain electrospinning conditions, adding just

Table 1 Fiber diameters (nm) determined by ImageJ analysis

Fiber diameter (nm)				
V (kV); *Q* (mL/h)	**PCLNs**	**PCLN_0.2PBE**	**PCLN_0.4PBE**	**PCLN_0.6PBE**
20 kV; 2 mL/h	111.99 ± 52.16^{cC}	172.55 ± 76.58^{aB}	173.74 ± 79.86^{aB}	253.38 ± 80.90^{abA}
25 kV; 2 mL/h	123.82 ± 48.22^{bcB}	195.26 ± 91.36^{aA}	195.21 ± 102.33^{aA}	225.43 ± 83.21^{bA}
20 kV; 1.6 mL/h	145.92 ± 50.05^{abC}	178.97 ± 67.65^{aB}	178.59 ± 52.92^{aB}	235.39 ± 92.46^{bA}
25 kV; 1.6 mL/h	159.06 ± 61.37^{aC}	188.74 ± 92.33^{aBC}	209.46 ± 75.76^{aB}	285.93 ± 131.38^{aA}

Columns with different lowercase letters differ statistically for electrospinning conditions ($p \leq 0.05$)

Rows with different uppercase letters differ statistically for PBE concentrations ($p \leq 0.05$)

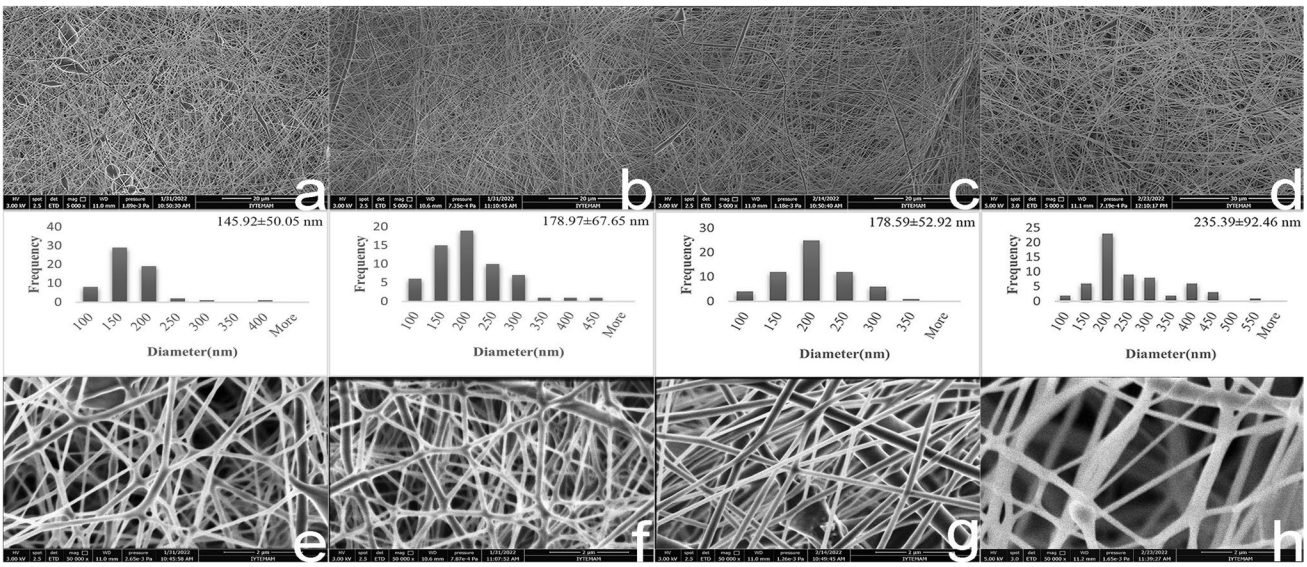


Fig. 2 **a**–**d** Raw SEM images (× 5000) and the diameter distributions, and **e**–**h** contrast-enhanced SEM images (× 50,000) of **a**, **e** PCLN; **b**, **f** PCLN_0.2PBE%; **c**, **g** PCLN_0.4PBE%, **d**, **h** PCLN_0.6PBE% where $V = 20$ kV; $Q = 1.6$ mL/h

0.2% (w/v) PBE resulted in bead-free nanofibers (Fig. S3), whereas the improvement was more noticeable at higher PBE concentrations (Figs. S4 and S5). Therefore, it can be concluded that incorporation of 0.2–0.4% (w/v) PBE to a 10% (w/v) PCL solution increased the viscosity to a critical level high enough to achieve bead-free nanofiber production. Table 1 shows the effect of PBE concentration on the fiber diameter. The fiber diameter increased in the order of PCLN < PCLN_0.2PBE ≈ PCLN_0.4PBE < PCLN_0.6PBE for all electrospinning conditions, which was perfectly in alignment with the order of increase in solution viscosity (Table S1). These findings indicate that the solution viscosity was the most critical factor in administering the diameter of nanofibers. The effect is due to the enhanced viscoelasticity of the polymer jet resulting in less capability to strech into small diameter nanofibers (Wen et al., 2022). Similar observations have been reported by others (Duan et al., 2021; Luiza et al., 2021; Moreira et al., 2019; Prietto et al., 2018; Sun et al., 2021). Lastly, the zoomed-in images of the nanofibers in Fig. 2e–h illustrate how the fiber structure and packing change with varying concentrations of PBE. The neat PCLN film features a densely interconnected network of primarily branched nanofibers. In contrast, as the PBE content increases, the fibers gradually lose their branched morphology and become more loosely packed. This decrease in fiber packing density is linked to the increase in fiber diameter with higher PBE concentrations; as the diameter of the fibers increases, the number of strands occupying a given area diminishes (Rahma et al., 2016). Other studies have also reported similar findings (Kaur et al., 2012; Varesano et al., 2009).

FT-IR Spectra of the Electrospun Films

The raw FTIR spectra obtained from lyophilized PBE powder and PCLN films, both with and without various concentrations of PBE, are presented in Fig. S6. As no meaningful differences were observed among the film samples containing PBE, only the spectra of the PBE powder and the PCLN_06PBE film are shown in Fig. 3 for clarity. The spectrum for PBE exhibited characteristic bands

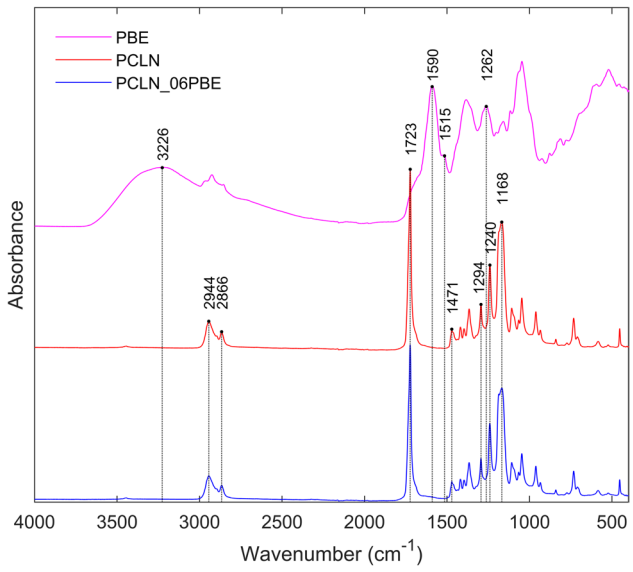


Fig. 3 FTIR spectra of PBE and PCLN nanofibrous films containing different PBE concentrations

for flavonoids. The broad band at 3226 cm^{-1} corresponds to the O–H stretching vibrations in the H-bonded hydroxyl groups (Bhushan et al., 2023; Gościniak et al., 2024; Guclu et al., 2023). The bands at 1590 cm^{-1} and 1515 cm^{-1} correspond to the C = C stretching vibrations (skeletal vibrations) in the aromatic ring (Bhushan et al., 2023; Gościniak et al., 2024; Guclu et al., 2023; Sarkar et al., 2021), whereas 1262 cm^{-1} band is ascribed to the phenol pyran ring stretching (Bhushan et al., 2023; Jovanska et al., 2022). It is also observed that PBE contains alkane groups in addition to aromatics; i.e., the peaks around 2900 cm^{-1} are attributed to the C-H stretching in the aliphatic structure (Guclu et al., 2023). It has been shown before that PBE used in this study contains additional compounds other than anthocyanins, such as chlorophylls (Erez & Bayramoglu, 2024).

The FTIR spectrum of the neat PCLN film was very similar to those obtained by other scholars in the literature (Kandi et al., 2021; Kotcharat et al., 2021; L. Liu et al., 2022; Solechan et al., 2022). The peaks at 2944 cm^{-1} and 2866 cm^{-1} correspond to the symmetric and asymmetric C-H stretching in alkanes, respectively (Jovanska et al., 2022; Liu et al., 2022), while the strong absorbance at 1723 cm^{-1} is for the C = O stretching vibration, a characteristic of PCL ester groups (Jovanska et al., 2022; Kandi et al., 2021; Solechan et al., 2022). The peak at 1471 cm^{-1} can be ascribed to C–C bending (Kotcharat et al., 2021). The bands at 1168 cm^{-1} and 1240 cm^{-1} are for the symmetric and asymmetric C–O–C stretching vibration in the ester bond (Kandi et al., 2021; Kotcharat et al., 2021; Liu et al., 2022). Additionally, the peak at 1294 cm^{-1} is attributed to the C–O and C–C stretching in crystalline phase (Kotcharat et al., 2021). The incorporation of PBE into the nanofibrous PCL film did not exhibit any significant shifts in wavenumbers, providing no clues for significant intermolecular interactions but caused slight reduction in intensities. This observation may be due to using very low amounts of PBE in the PCL solutions, as hydrogen bonding between the hydroxyl groups of anthocyanin molecules and ester group of PCL is very likely to occur (Liu et al., 2022). However, a shoulder appearing at 1590 cm^{-1} (skeletal vibrations in the aromatic ring) in the IR spectrum of PCLN_06PBE provides strong evidence that PBE was successfully incorporated into the nanofibrous PCL film, as no absorption was detected at this band for the neat PCLN film.

Thermal Analysis of the Electrospun Films

The thermal properties of PBE, PCL pellets, and the nanofibrous films (PCLN, PCLN_0.4PBE, and PCLN_0.6PBE) were characterized by DSC and TGA analyses. The corresponding thermal profiles are shown in Fig. 4, whereas the thermal parameters are summarized in Table S2. For PBE, the broad endothermic peak at ~ 75 °C tailing up to around 115 °C (Fig. 4a) can be attributed to the desorption of water or other volatile compounds from the lyophilized extract, whereas the small peak around 130 °C likely corresponds to the breakage of hydrogen bonds between the components in the extract (Dos Santos et al., 2023) and, therefore, to the beginning of the decomposition process, as also suggested by TGA analysis (Fig. 4b). The characteristic endothermic peak corresponding to the melting temperature (T_m) of PCL was observed around 60 °C in the pellet form, which shifted to the left (~ 58 °C) in the nanofibrous PCLN (Fig. 4a). Additionally, the heat of fusion (ΔH_m) decreased from 49.03 ± 7.91 J/g (in PCL pellet) to 41.65 ± 0.18 J/g in the nanofibrous PCLN film. These changes indicate that the nanofibrous PCLN film has lower crystallinity than PCL in pellet form. Compared with the PCLN film, a small decrease in both the onset temperature and melting

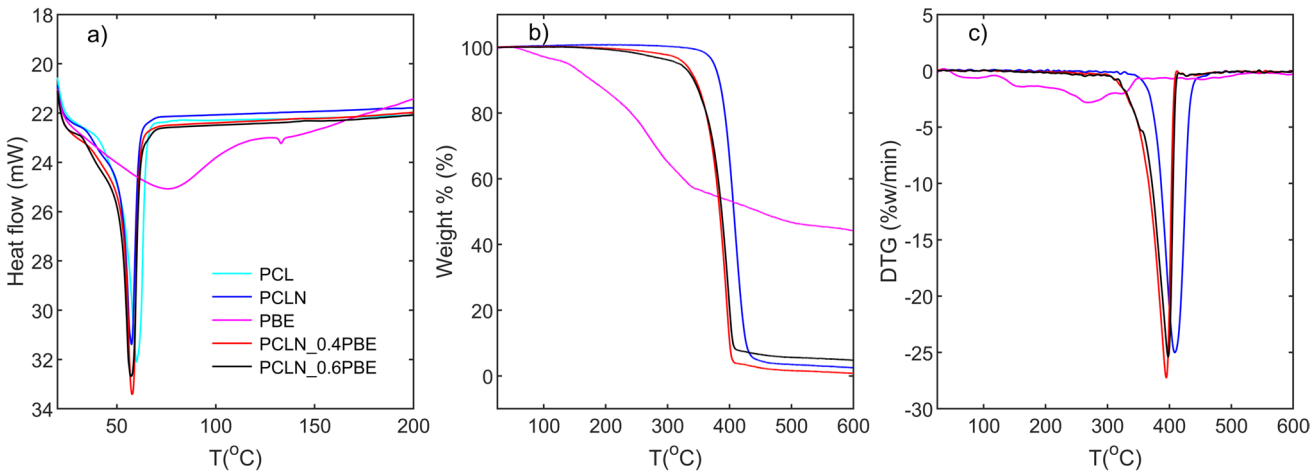


Fig. 4 **a** DSC, **b** TGA, **c** DTG profiles of PBE, PCL, electrospun PCLN, PCLN_0.4PBE, and PCLN_0.6PBE films

temperature was observed in PCLN_0.6PBE, suggesting a weak reduction in crystallinity with the incorporation of PBE into the nanofibers. These results suggest good miscibility between PCL and PBE in the fabricated films, in accordance with the results of other similar studies (Shi et al., 2022; Zou et al., 2023).

The TGA thermogram (Fig. 4b) represents the residual weight percent of the samples as a function of temperature, whereas the DTG profile (Fig. 4c) gives the samples' rate of weight change (dW/dt) with respect to temperature. These profiles give information about the thermal degradation behavior of the samples. PBE exhibited several stages of weight loss, whereas the nanofibrous films exhibited a single stage. The first stage between 25 and 115 °C corresponds to the desorption of water and other volatiles from the extract. The thermal decomposition of PBE starts beyond 120 °C. The first, second, and the third stages of thermal decomposition occurred between 120–220 °C, 220–300 °C, and 300–520 °C, respectively. The temperature at 10% weight loss ($Td_{10\%}$) and at the maximum weight loss rate (Td_{max}) of crude PBE were determined as ~ 177 °C and ~ 263 °C, respectively, while its residual weight percent was found as 44% (Table S2). These results follow closely to the thermal degradation profile of cyanidin-3-O-glucoside (Dong et al., 2022). Neat PCL nanofibrous films exhibited values of ~ 383 °C and 408 °C for $Td_{10\%}$ and Td_{max}, respectively. These findings are in agreement with those of Silva et al. (2019), who determined, respectively, the initial and maximum degradation rate temperatures of nanofibrous PCL films (electrospun from 11% w/w PCL solution) as 356 °C and 405 °C. The incorporation of PBE into the electrospun films decreased the $Td_{10\%}$ value to 342–345 °C and Td_{max} value to 395–398 °C for both PCLN_0.4PBE and PCLN_0.6PBE films. This finding indicates a slight reduction in the thermal stability of nanofibrous PCL films upon the addition of PBE, which aligns with the observed decrease in their crystallinity. Similarly, Silva et al. (2019) observed a slight decrease in the initial and maximum degradation temperatures of electrospun PCL films upon the addition of açaí extract. Moreira et al. (2018) also observed a reduction in these parameters for electrospun PLA/PEO films with the incorporation of 2–6% phycocyanin.

Mechanical Characterization

The mechanical properties of electrospun films fabricated with and without PBE at a voltage of 20 kV and a flow rate of 1.6 mL/h are detailed in Table 2. The TS values decreased from 4.90 ± 2.67 MPa to 2.47 ± 0.34 MPa, with increasing PBE content. These low TS values are typical of electrospun mats due to high porosity and looser interconnected network of fibers (Forghani et al., 2021). The reduction in the films' TS with the incorporation of PBE can be explained based on both the decrease in film thickness and fiber packing density. The film thickness decreased from 122.10 ± 14.40 µm to 95.60 ± 19.59 µm, which opposed the increase in fiber diameter from 145.2 ± 50.05 nm to 235.39 ± 92.46 nm (see the "Morphological Characteristics" section). The increase in fiber diameter resulted in a lower fiber packing density, leading to a looser network of interconnected fibers, as demonstrated by the SEM images (Fig. 2e–h). This change reduced the mechanical resistance of the films. These findings are consistent with those of Conte et al. (2020), who showed that increasing film thickness and denser fiber packing improved the mechanical properties of nanofibrous PCL films. They attributed this effect to enhanced fiber–fiber junctions and interactions, which increased friction among them. Other studies have yielded similar results. Duan et al. (2021) reported that incorporating curcumin and anthocyanin into pullulan-chitin films led to decreased TS. Additionally, Shavisi and Shahbazi (2022) observed reduced TS values in chitosan-gum Arabic nanofiber membranes by the addition of *Rosa damascena* extract. The authors explained these effects by highlighting the role of hydrogen bonds and/or hydrophobic interactions associated with the phenolic compounds in the extract, which diminished the intermolecular interactions between polymer chains and resulted in greater inter-chain distances within the chitosan-gum Arabic network. Since FTIR analysis indicated no apparent intermolecular interactions between PBE and PCL nanofibers—likely due to the very low concentrations of PBE used ("FT-IR Spectra of the Electrospun Films" section)—the explanation regarding fiber packing density as the cause of the reduced mechanical resistance in our films is more plausible.

The addition of PBE significantly increased the flexibility of the PCLN film, as indicated by the increase in EB values.

Table 2 The mechanical properties of nanofibrous films fabricated at a voltage of 20 kV and a flow rate of 1.6 mL/h

	Film thickness (µm)	Tensile strength (TS) (MPa)	Elongation at break (EB) (%)	Young's modulus (YM) (MPa)
PCLN	122.10 ± 14.40^{a}	4.90 ± 2.67^{a}	55.46 ± 11.29^{b}	0.11 ± 0.05^{a}
PCLN_0.4PBE	108.80 ± 15.05^{ab}	3.80 ± 0.99^{ab}	82.26 ± 21.79^{a}	0.09 ± 0.01^{a}
PCLN_0.6PBE	95.60 ± 19.59^{b}	2.47 ± 0.34^{b}	85.15 ± 19.36^{a}	0.08 ± 0.01^{a}

Columns with different lowercase letters differ statistically for different PBE concentration ($p \leq 0.05$) ($n = 8$)

This suggests that PBE acted as a plasticizer, enhancing the mobility of PCL chains. This effect may be attributed to the presence of other types of polysaccharides in the crude extract of purple basil, which could have weakened the interactions between polymer chains (Freitas et al., 2020). However, the influence of PBE concentration on EB was found to be statistically insignificant within the concentration range studied in this work. These findings are consistent with those of other researchers (Duan et al., 2021; Shavisi & Shahbazi, 2022). Finally, the YM values were not affected by the presence or concentration of PBE, suggesting that PBE did not impact the stiffness of the nanofibrous PCL film, at least at the low concentrations used in this study.

Water Contact Angle (WCA) Analysis

PCL is a chemically hydrophobic polymer that is commonly used as a base for creating water-resistant materials. This property helps protect nanofibrous films from collapsing or dissolving when they come into contact with liquid samples. However, while hydrophobic polymers maintain the structural integrity of the indicator film, they also decrease the films' reaction sensitivity. This is because the color transformation mechanism of anthocyanins requires the presence of ionized water (Zhang et al., 2022). Therefore, an effective colorimetric pH indicator film must possess sufficient hydrophilicity to promote water spreading on its surface and facilitate diffusion through its matrix.

In this study, WCA analysis was utilized to evaluate the wettability of the electrospun films. A surface that is hydrophobic typically exhibits a WCA higher than 90°, preserving the shape of water droplets, whereas surfaces with a WCA lower than 90° display hydrophilic characteristics. Wetting, i.e., spreading of a water droplet on a surface, occurs on hydrophilic surfaces, and complete wetting yields a WCA of 0° (Yuan & Lee, 2013). As illustrated in Fig. 5, the WCA of PCL nanofibers showed hydrophobic properties, indicated by a measurement of around 90°, with no significant wetting observed over time. In contrast, PCLN_0.4PBE and PCLN_0.6PBE films displayed hydrophilic characteristics, as wetting gradually occurred over time, ultimately resulting in complete wetting. Furthermore, PCLN_0.6PBE exhibited greater hydrophilicity than PCLN_0.4PBE, as the absorption of water droplets occurred significantly faster with PCLN_0.6PBE. The hydrophilicity of electrospun membranes is influenced by several factors, including surface chemistry and morphology, porosity, the diameters of the ultrafine fibers, and capillary action within the membrane (Prietto et al., 2018). Each of these aspects contributes to the membrane's ability to attract and retain moisture. The improved wettability of our films with increasing PBE content can be attributed to both changes in chemical composition and structural modifications within the fiber network.

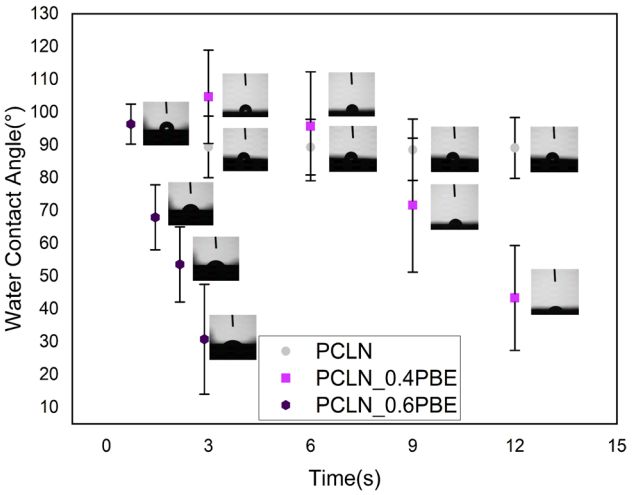


Fig. 5 Water contact angle values of PCLN, PCLN_0.4PBE, and PCLN_0.6PBE films as a function of time

Lv and colleagues (2024) stated that there is a large number of hydrophilic hydroxyl groups on the molecular chain of Roselle anthocyanin; thus, incorporating anthocyanin had a specific hydrophilicity-enhancing effect on the mats. Not surprisingly, integrating anthocyanin-rich PBE into PCL nanofibers yielded a similar effect in this study, despite the relatively low concentrations explored. Additionally, it was shown in the "Morphological Characteristics" section that increasing the PBE content resulted in thicker fibers and a lower fiber packing density in the nanofibrous films. This structural change in the fiber network likely significantly increases the water absorption rate of the film, thereby enhancing its hydrophilicity. It is known that higher fiber density typically leads to increased surface roughness, which enhances the air entrapment between fibers (Szewczyk et al., 2018). This results in a reduction of surface free energy, higher WCA values, and slower water absorption rates (Kopeć et al., 2020). Conversely, a looser fiber network created by adding PBE reduces the entrapment of air between fibers, allowing for better liquid–solid interaction and improved water absorption.

Our findings are supported by the results of several scholars in the literature. Nur and Parın (2022) found that the WCA of the thermoplastic polyurethane and polycaprolactone film decreased with the addition of spirulina. Incorporating 1 wt% spirulina improved the hydrophilicity of the composite nanofibers by reducing WCA to ~ 36°. Similarly, Jovanska and colleagues (2022) reported that adding PEO and *Hibiscus rosa sinensis* extract into PCL solution enhanced the hydrophilic characteristics of the resulting membranes. The WCA of all samples studied was less than 90° (Jovanska et al., 2022). Silva et al. (2019) showed that the WCA of nanofibrous films fabricated using a blend of PCL/PEO was 30.25 ± 4.32°, whereas WCA was measured

as 122.34 ± 1.72° for nanofibrous mats made from PCL. Guclu et al. (2023) also observed that anthocyanin incorporation into PCL/PEG solution reduced WCA values of the PCL/PEG nanofibers, making them more hydrophilic. Lastly, in line with our study, Prietto et al. (2018) reported that the nanofiber mats of zein with 5% anthocyanin exhibited a WCA of 0° in just 2 s, while zein with 4%, 3% anthocyanin, and pure zein films achieved the same in with 4, 5, and 10 s, respectively. The authors explained that the increased hydrophilicity makes the diffusion of H + or OH– into the fibers easier, allowing these ions to interact with anthocyanin molecules, which results in a consequent rapid color-change response to pH change.

Colorimetric pH Indicator Performance of the Nanofibrous Films

The most crucial attribute of colorimetric pH indicator packaging is its color change response to the variation in environmental pH. It is important for this response to be rapid and easily distinguishable by the naked eye (Forghani et al., 2021). In this work, the color change response of the fabricated nanofibrous films was tested against aqueous solutions having different pH, gelatin gels at pH 2.5/11 simulating semi-solid acidic/alkaline foods, and volatile ammonia. The latter evaluation is critical in determining the suitability of the material for use in the packaging of fresh meat products.

The films were initially tested against aqueous pH buffer solutions. Based on the results in the "Morphological Characteristics" section, only the films fabricated at conditions yielding the most bead-free, small-diameter, and uniform fiber morphology (V = 20 kV, Q = 1.6 mL/h) were subjected to buffer solutions with varying pH values (1–10). The methodology described in the "Color Change Response of Electrospun Films to Various pH Buffers, Ammonia Vapor, and Gelatin Gels at Different pH Values Simulating Semi-solid Foods" section was used to assess the films' total color change (ΔE) response to pH. The corresponding images for all films and the calculated ΔE values for PCLN_0.4PBE and PLCN_0.6PBE films are provided in Tables 3 and 4, respectively. As expected, the control films did not exhibit any noticeable color change in response to pH variations, while the films incorporating PBE changed from light mulberry at pH 1 to grayish-green at pH 10, consistent with the color change of aqueous PBE solution with pH (Erez & Bayramoglu, 2024). The performance of PCLN_0.4PBE and PCLN_0.6PBE films was superior to that of PCLN_0.2PBE in terms of both the total color change between successive pH changes and the response time. The time required to observe a noticeable color change in PCLN_0.2PBE was around 5 min, whereas it took only 4–5 s for the others. The response time of similar nanofibrous pH-indicator films in the literature was around 3–5 s (Agarwal et al., 2012; Prietto et al., 2018; Zhang et al., 2011). Therefore, PCLN_0.2PBE films may not be suitable as an efficient pH-indicator material because of their slow response time. This is why PCLN_0.2PBE films were excluded from further analyses. Regarding the total color change response of PCLN_0.4PBE and PCLN_0.6PBE films to variations in pH, it was observed that they exhibited comparable performance. In Table 4, note that the numbers given in the diagonals of the matrices correspond to ΔE response of the films to successive pH changes, i.e., a unit change in pH. For instance, the values reported in the intersection of the first row (pH 1) and first column (pH 2) correspond to ΔE response of the films at pH 2 with respect to the color parameters at pH

Table 3 Photographs of the nanofibrous films fabricated at V = 20 kV and Q = 1.6 mL/h using 10% (w/v) PCL with different PBE concentrations

PBE (% w/v)	pH 1	pH 2	pH 3	pH 4	pH 5	pH 6	pH 7	pH 8	pH 9	pH 10
0										
0.2										
0.4										
0.6										

Table 4 Color change (ΔE) values for PCLN_0.4PBE and PCLN_0.6PBE fabricated at $V = 20$ kV and $Q = 1.6$ mL/h

PCLN_0.4PBE									
*pH	2	3	4	5	6	7	8	9	10
1	2.33 ± 0.17	4.04 ± 0.35	7.84 ± 2.20	12.65 ± 1.53	16.11 ± 1.72	17.81 ± 1.22	19.49 ± 1.54	24.06 ± 2.69	25.19 ± 3.13
2		1.80 ± 0.26	5.72 ± 2.24	10.63 ± 1.59	14.07 ± 1.79	15.70 ± 1.23	17.39 ± 1.55	22.12 ± 2.81	23.36 ± 3.30
3			4.00 ± 1.90	8.94 ± 1.23	12.33 ± 1.47	13.92 ± 0.97	15.62 ± 1.31	20.40 ± 2.54	21.72 ± 2.96
4				4.97 ± 0.65	8.45 ± 0.37	10.20 ± 0.83	12.04 ± 0.38	16.65 ± 0.75	17.90 ± 1.23
5					3.64 ± 0.24	5.89 ± 0.34	7.89 ± 0.15	11.88 ± 1.29	12.98 ± 1.93
6						2.72 ± 0.44	4.65 ± 0.00	8.32 ± 1.06	9.74 ± 1.58
7							2.07 ± 0.54	7.16 ± 1.65	9.48 ± 1.60
8								6.10 ± 1.39	8.95 ± 1.10
9									3.56 ± 0.92
PCLN_0.6PBE									
*pH	2	3	4	5	6	7	8	9	10
1	3.92 ± 3.11	4.43 ± 1.39	10.02 ± 1.40	11.95 ± 1.41	16.06 ± 0.44	16.20 ± 1.15	18.69 ± 1.80	22.80 ± 1.83	24.23 ± 1.91
2		1.85 ± 0.87	6.89 ± 2.71	8.81 ± 2.41	12.99 ± 3.45	13.12 ± 2.17	15.44 ± 1.77	20.07 ± 1.45	21.33 ± 1.80
3			6.12 ± 0.52	7.93 ± 0.32	12.10 ± 1.36	12.07 ± 0.31	14.50 ± 0.26	19.01 ± 0.34	20.49 ± 0.22
4				2.54 ± 0.25	6.25 ± 0.78	7.38 ± 0.07	9.34 ± 0.07	13.86 ± 1.36	14.83 ± 0.65
5					4.25 ± 1.13	5.01 ± 0.16	6.97 ± 0.25	11.55 ± 1.29	12.65 ± 0.61
6						3.78 ± 0.74	4.27 ± 0.64	7.98 ± 2.31	8.85 ± 1.36
7							2.89 ± 1.20	7.53 ± 0.41	9.79 ± 0.69
8								6.24 ± 0.76	7.59 ± 0.48
9									4.59 ± 3.18

*The numbers given in the diagonals of the matrices correspond to ΔE response of the films to successive pH changes

1 taken as a reference. On the other hand, to evaluate the color change of the films at pH 4 in going from pH 2 to 4, one should read the value in the intersection of the second row (pH 2) and the third column (pH 4) of the corresponding table. According to Mokrzycki and Tatol (2011), the human eye cannot perceive a color difference when the ΔE value is below 1; only trained observers can discern a difference when the ΔE value falls between 1 and 2; inexperienced observers can detect a color variance between 2 and 3.5; the color difference is clear for ΔE values between 3.5 and 5; and any observer can easily notice different colors for ΔE values greater than 5. In this context, both films displayed color responses to successive pH changes that were at least noticeable by inexperienced observers (except for the pH change from 2 to 3). The color response of PCLN_0.4PBE to successive pH changes in the range from 4 to 6 and from 9 to 10 fell within the clearly-noticed category, while the same can be said for PCLN_0.6PBE's response to pH changes in the ranges of 4, 6–7, and 9–10. It is important to note that the pH range of 5 to 8 is critical for the deterioration of most food products (Prietto et al., 2017). This includes low-acid foods such as meat, poultry, fish, dairy products, and both cooked and some raw vegetables, as well as relatively neutral foods like eggs. Preserving low-acid foods is particularly challenging because their pH levels are conducive to the growth of several vegetative bacterial pathogens (Houška et al., 2022). Therefore, it is crucial for a pH indicator material to show clearly noticed color changes to a unit change in pH level within the range of 5 to 7. Additionally, both films exhibited excellent color change values ($\Delta E > 5$) that can be easily noticed by any observer for pH variations of at least two units. Consequently, both films show promising results as potential colorimetric pH indicators.

Next, the performance of PCLN_0.4PBE and PCLN_0.6PBE films was tested against volatile ammonia. According to Dong et al. (2020), ammonia is one of the biogenic amines produced during the decay of protein-rich foods, which gradually creates an alkaline environment in the package. The study suggests that if the electrospun nanofiber films show a color change when exposed to ammonia vapor, they can be used to monitor the freshness of fish or meat products. The responses of PCLN_0.4PBE and PCLN_0.6PBE films to the vapor of a 0.8 M ammonia solution as a function of time are presented in Fig. 6. Both films changed color from light pink to light yellow in 15 min and then to yellow at the end of a 30-min reaction. PCLN_0.6 PBE exhibited an easily noticeable color change with a ΔE of ~ 5 in only 5 min of exposure to ammonia vapor, whereas PCLN_0.4PBE showed a similar colorimetric change for over 15 min. The ΔE values of PCLN_0.6PBE and PCLN_0.4PBE films were 13.23 ± 1.26 and 8.57 ± 0.03, respectively, at the end of 30-min

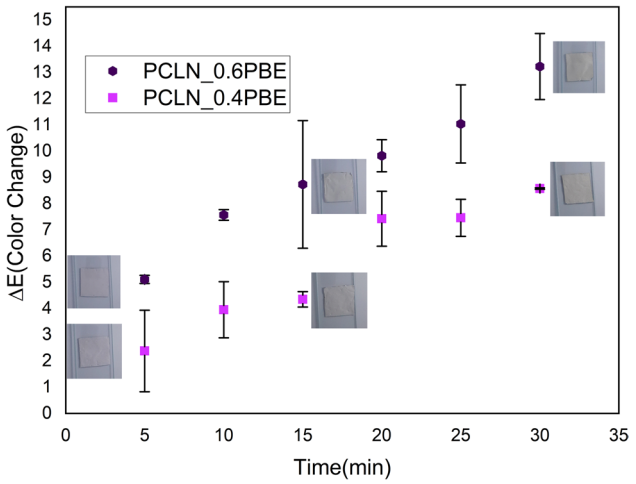


Fig. 6 Total color change (ΔE) of PCLN_0.4PBE and PCL_0.6PBE to 0.8 M ammonia solution as a function of time

reaction. Increasing PBE concentration in the film resulted in a more pronounced colorimetric response in a shorter time. This observation is consistent with the results of Freitas et al. (2020), who showed that increased contents of red cabbage extract in cellulose acetate films led to quicker and more substantial color transformations, as well as several other studies (He et al., 2023; Jang et al., 2023; Kang et al., 2020; Liu et al., 2023; Shi et al., 2023). The effect of exposure time was also positive on the colorimetric response of the films. Shi et al. (2023) explained this effect based on the increased concentration of ammonia vapor released from the solution with prolonged exposure, which can adsorb on the surface and diffuse into the films to a greater extent. The subsequent hydrolization of volatile ammonia into hydroxyl ions induces the formation of an alkaline environment, which triggers the structural transformations in the anthocyanin-rich extract, leading to the color transitions. Our results suggest that PCLN_0.6PBE films may be a better option for food packaging of fresh meat or fish, as they can effectively detect ammonia vapor in a shorter time. However, it is essential to apply these films to real food materials in order to fully evaluate their effectiveness in detecting the biogenic amines released into the headspace during the deterioration of the food products.

Finally, the performance of the films was evaluated against gelatin gels prepared at pH 2.5 and pH 11, which represent acidic and alkaline semi-solid foods, respectively. Both films displayed significant color changes after 15 min of contact with the gels, and these changes remained relatively stable after 30 min, despite some uncertainties, as shown in Fig. 7. The ΔE responses of the PCLN_0.4PBE and PCLN_0.6PBE samples to the acidic gels after 15 min were recorded as 8.82 ± 2.55 and 23.74 ± 3.42, respectively. The color change observed was from light pink to a darker pink, with the effect being more pronounced in the PCLN_0.6PBE sample. In contrast, when in contact with alkaline gels, the color shifts for the PCLN_0.4PBE and PCLN_0.6PBE films changed from light pink to dark greyish-green, with their respective ΔE responses at 15 min recorded as 13.02 ± 1.90 and 20.43 ± 6.30. Increasing the concentration of PBE in the films resulted in a more pronounced colorimetric response in both acidic and alkaline conditions, similar to the observations from the volatile ammonia analysis. However, the standard deviations also increased, likely due to the higher inhomogeneity in fiber diameter (Table 1) and film thickness (Table 2) as well as increased wettability seen in the PCLN_0.6PBE films ("Water Contact Angle (WCA) Analysis" section). Due to the latter effect, the moisture from the gel likely permeates the films, potentially leading to localized swelling, dilution, or uneven distribution of PBE within them.

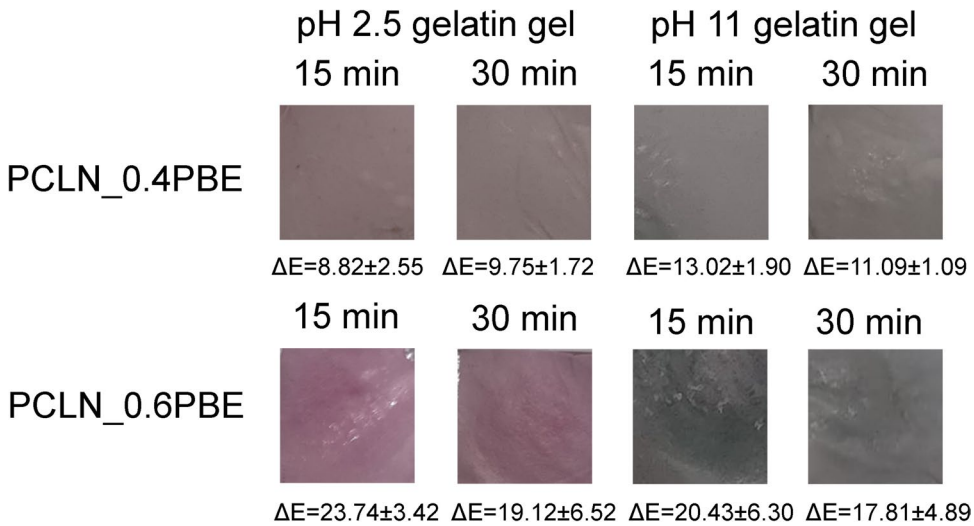


Fig. 7 Total color change (ΔE) of PCLN_0.4PBE and PCNL_0.6PBE to gelatin gels prepared at pH 2.5 and pH 11

Color Stability of the pH Indicator Films

The stability of anthocyanins can be affected by various factors such as pH, temperature, humidity, and light (He et al., 2023). In this study, the color stability of nanofibrous films containing PBE was evaluated during storage for 28 days under extreme humidity conditions (75% RH) at 25 °C and 4 °C in the dark. The same criterion as in the "Colorimetric pH-Indicator Performance of the Nanofibrous Films" section was used to assess the color change, where a color difference is considered "clear" for $\Delta E > 3.5$. The results are presented in Fig. 8. As expected, the color stability of the films was highly dependent on temperature. Films stored at 4 °C exhibited higher color stability than those stored at 25 °C. It is well-known that higher temperatures accelerate the oxidation of anthocyanin molecules (Zhai et al., 2018). Both PCLN_0.6PBE and PCLN_0.4PBE films stored at 4 °C maintained a ΔE value below 3.5 for up to 14 days, indicating good color stability for 2 weeks. Conversely, none of films could maintain stability after 3–4 days of storage at 25 °C. Additionally, the color stability at 25 °C varied with PBE concentration; the PCLN_0.6PBE film exhibited accelerated color loss after 14 days compared to PCLN_0.4PBE. However, there was no significant difference in the color change behavior of both films stored at 4 °C. The accelerated loss of color stability at 25 °C in films with higher PBE content can be attributed to their increased anthocyanin levels and enhanced hydrophilicity (see "Water Contact Angle (WCA) Analysis" section). It is important to note that extreme humidity conditions were present during the storage test. Overall, both films show promising potential for applicability as a pH indicator on foods stored under refrigeration in the dark, with good color stability for up to 14 days.

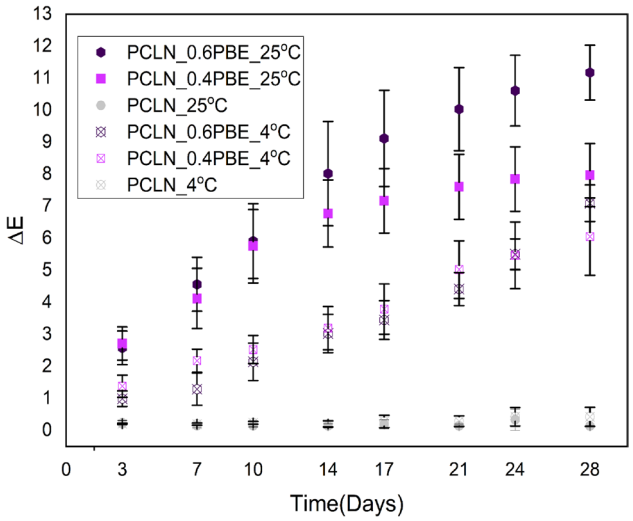


Fig. 8 Total color change (ΔE) of the PCLN, PCLN_0.4PBE, and PCLN_0.6PBE during storage under 75% RH at 4 °C or 25 °C

Release Assays

The release of the colorimetric pH indicator material from the intelligent packaging is not favorable because the migration of the colorant causes efficiency loss and unwanted color changes in the food. The rate of PBE release from the nanofibrous films was determined in distilled water (DW), 3% acetic acid (AcAc), and 50% ethanol (EtOH), representing hydrophilic foods with a pH above 4.5, acidic aqueous, and lipophilic foods, respectively. Figure 9 shows that the rate of PBE release from the colorimetric pH indicator films depends on the nature of the food simulant. The PBE release was maximum in 50% ethanol, followed by distilled water, while it was minimum (almost zero) in 3% acetic acid. Similar release trends were observed for the PCLN_0.4PBE and PCLN_0.6PBE samples in all food simulants, taking into account the ranges of uncertainty. Moreover, the release behavior did not change significantly with respect to temperature. An initial burst release within 30 min was observed in both EtOH and DW media, followed by a sustained release period. The burst release is typically due to the presence of the extract on or near the nanofiber surface that releases quickly upon the swelling of the matrix with exposure to the release medium (Atay et al., 2018). The results indicate that the release is accelerated when the films are in contact with 50% ethanol, which can be attributed to the hydrophobic nature of PCL. Ethanol has a moderate polarity; therefore, it has a higher affinity for the hydrophobic PCL chains than water, which facilitates the absorption and swelling. Bridge et al. (2002) showed that pretreatment of hydrophobic PAN-PVC membranes with ethanol increased the permeability and ultrastructure of the membrane, most likely due to the increased chain mobility, which is a characteristic of swollen polymer systems. Hirano et al. (2021) also showed that the hydrophilicity of PCL sheets was enhanced upon pretreatment with 70% ethanol. Overall, the results suggest that the loss of colorimetric pH indicator extract from the nanofibrous PCL films is expected to be the highest when in contact with lipophilic foods, whereas it is expected to be minimal when in contact with acidic foods.

Conclusion

Intelligent packaging plays a vital role in enhancing food safety, evaluating food quality, and reducing waste. This study focused on the development of potential colorimetric pH indicator films using PCL integrated with PBE via electrospinning for the first time. The effects of PBE content, voltage, and flow rate on fiber morphology were analyzed. The films were characterized based on their chemical, thermal, mechanical, and wetting properties and their color change response to pH, color stability, and PBE release rate.

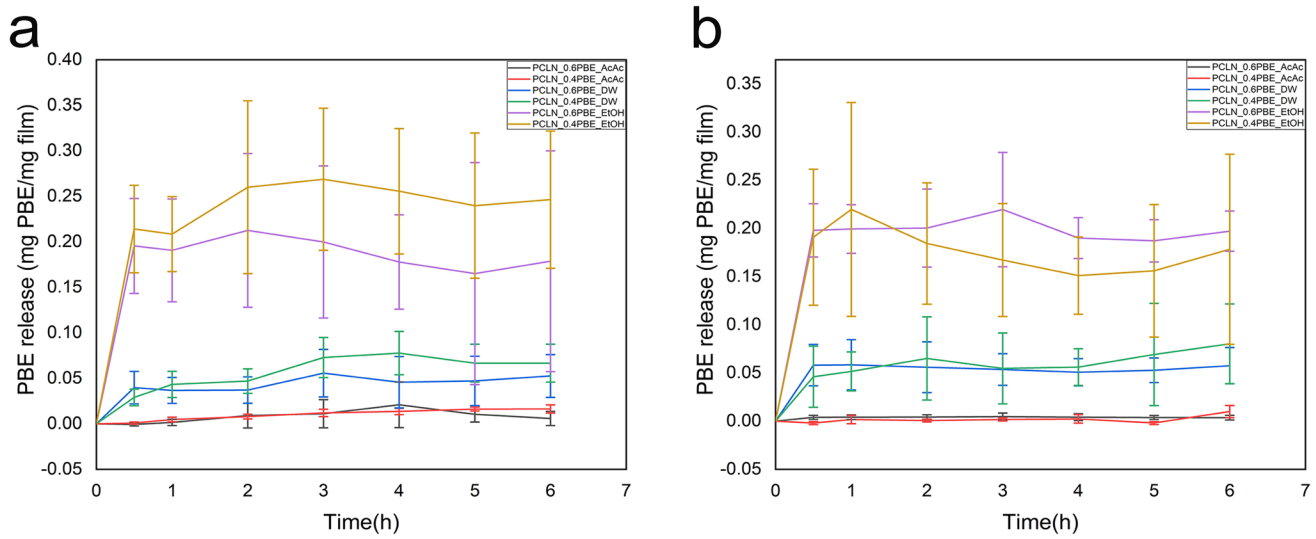


Fig. 9 Time-dependent PBE release from the PCLN_0.4PBE and PCLN_0.6PBE films into different food simulants at **a** 4 °C and **b** 25 °C. AcAc, DW, and EtOH stand for 3% acetic acid solution, distilled water, and 50% ethanol solution, respectively

The results show that PCL films with 0.4% and 0.6% PBE displayed notable color transitions in response to successive pH changes in aqueous media, gelatin gels that simulate acidic and alkaline semi-solid foods, and volatile ammonia, with the higher concentration film performing better. At room temperature, both films maintained color stability for up to 4 days, and up to 14 days when refrigerated and kept dark, offering a potential early warning for food poisoning. The release assays showed the highest PBE release in 50% ethanol, with minimal release in acidic conditions, indicating resistance to acidic foods. PBE incorporation enhanced wettability and flexibility of the films, though it slightly reduced thermal stability and decreased mechanical resistance. Overall, our findings suggest that nanofibrous PCL films integrated with PBE have promising potential to monitor food spoilage for refrigerated items like cheese, fish, seafood, and meat products over a period of up to 14 days. Further research is needed to thoroughly assess their performance with specific food products. This study highlights the advantages of utilizing electrospinning to create films from hydrophobic polymers that possess self-integrity while ensuring sufficient wettability, allowing for a rapid response to environmental pH changes, even with very low amounts of extracts.

Supplementary Information The online version contains supplementary material available at https://doi.org/10.1007/s11947-025-03903-9.

Acknowledgements We greatly acknowledge Özen&Tokatlı Lab, Korel Lab, Özdemir Lab, IZTECH Composite Materials Laboratory, and IZTECH Integrated Research Center for appliance support during the experiments. We are specifically grateful to Yekta Günay Atlı, Murat Delman, Evrim Paşık, Burcu Akdağ Çağlar, and Zehra Sinem Yılmaz in IZTECH Integrated Research Center.

Author Contribution E.E: conceptualization, data curation, methodology, investigation, software, validation, formal analysis, visualization, writing-original draft preparation. A.E.E: methodology, resources, writing-review. B.B: conceptualization, methodology, project administration, resources, writing-review and editing.

Funding Open access funding provided by the Scientific and Technological Research Council of Türkiye (TÜBİTAK).

Data Availability No datasets were generated or analysed during the current study.

Declarations

Conflict of Interest The authors declare no competing interests.

Open Access This article is licensed under a Creative Commons Attribution 4.0 International License, which permits use, sharing, adaptation, distribution and reproduction in any medium or format, as long as you give appropriate credit to the original author(s) and the source, provide a link to the Creative Commons licence, and indicate if changes were made. The images or other third party material in this article are included in the article's Creative Commons licence, unless indicated otherwise in a credit line to the material. If material is not included in the article's Creative Commons licence and your intended use is not permitted by statutory regulation or exceeds the permitted use, you will need to obtain permission directly from the copyright holder. To view a copy of this licence, visit http://creativecommons.org/licenses/by/4.0/.

References

Agarwal, A., Raheja, A., Natarajan, T. S., & Chandra, T. S. (2012). Sensors and actuators B : Chemical development of universal pH sensing electrospun nanofibers. *Sensors & Actuators: B. Chemical, 161*(1), 1097–1101. https://doi.org/10.1016/j.snb.2011.12.027

Alizadeh-Sani, M., Tavassoli, M., McClements, D. J., & Hamishehkar, H. (2021). Multifunctional halochromic packaging materials: Saffron petal anthocyanin loaded-chitosan nanofiber/methyl cellulose matrices. *Food Hydrocolloids, 111*, 106237. https://doi.org/10.1016/j.foodhyd.2020.106237

Aman Mohammadi, M., Hosseini, S. M., & Yousefi, M. (2020). Application of electrospinning technique in development of intelligent food packaging: A short review of recent trends. *Food Science and Nutrition, 8*(9), 4656–4665. https://doi.org/10.1002/fsn3.1781

Atay, E., Fabra, M. J., Martínez-Sanz, M., Gomez-Mascaraque, L. G., Altan, A., & Lopez-Rubio, A. (2018). Development and characterization of chitosan/gelatin electrosprayed microparticles as food grade delivery vehicles for anthocyanin extracts. *Food Hydrocolloids, 77*, 699–710.

Azari, A., Golchin, A., Maymand, M. M., Mansouri, F., & Ardeshirylajimi, A. (2021). Electrospun polycaprolactone nanofibers: Current research and applications in biomedical application. *Advanced Pharmaceutical Bulletin, 12*(4), 658. https://doi.org/10.34172/apb.2022.070

Barkhordari, M., Mohseni-Shahri, F. S., & Moeinpour, F. (2024). Bio-based gelatin–TiO2–purple basil extract nanocomposite films for monitoring fish freshness. *Journal of Food Measurement and Characterization, 18*(4), 2965–2976. https://doi.org/10.1007/s11694-024-02377-1

Bhushan, B., Bibwe, B., Pal, A., Mahawar, M. K., Dagla, M. C., Kr, Y., et al. (2023). FTIR spectra, antioxidant capacity and degradation kinetics of maize anthocyanin extract under variable process conditions. *Applied Food Research, 3*(1), 100282.

Bridge, M. J., Broadhead, K. W., Hlady, V., & Tresco, P. A. (2002). Ethanol treatment alters the ultrastructure and permeability of PAN-PVC hollow fiber cell encapsulation membranes. *Journal of Membrane Science, 195*(1), 51–64.

Cipitria, A., Skelton, A., Dargaville, T. R., Dalton, P. D., & Hutmacher, D. W. (2011). Design, fabrication and characterization of PCL electrospun scaffolds - A review. *Journal of Materials Chemistry, 21*(26), 9419–9453. https://doi.org/10.1039/c0jm04502k

Conte, A. A., Sun, K., Hu, X., & Beachley, V. Z. (2020). Effects of fiber density and strain rate on the mechanical properties of electrospun polycaprolactone nanofiber mats. *Frontiers in Chemistry, 8*, 610.

da Silva, C. K., da Silveira Mastrantonio, D. J., Costa, J. A. V., & de Morais, M. G. (2019). Innovative pH sensors developed from ultrafine fibers containing açaí (Euterpe oleracea) extract. *Food Chemistry, 294*, 397–404. https://doi.org/10.1016/j.foodchem.2019.05.059

de Oliveira Filho, J. G., de Oliveira Silva, C., do Canto, R. A., Egea, M. B., Tonon, R. V., Paschoalin, R. T., et al. (2024). Fast and sustainable production of smart nanofiber mats by solution blow spinning for food quality monitoring: Potential of polycaprolactone and agri-food residue-derived anthocyanins. *Food Chemistry, 457*, 140057. https://doi.org/10.1016/j.foodchem.2024.140057

Dong, H., Ling, Z., Zhang, X., Zhang, X., Ramaswamy, S., & Xu, F. (2020). Smart colorimetric sensing films with high mechanical strength and hydrophobic properties for visual monitoring of shrimp and pork freshness. *Sensors and Actuators b: Chemical, 309*, 127752.

Dong, J., Li, S., Zhang, J., Liu, A., & Ren, J. (2022). Thermal degradation of cyanidin-3-O-glucoside: Mechanism and toxicity of products. *Food Chemistry, 370*, 131018.

Dos Santos, F. N., De Souza, E. J. D., De Souza, J. F., Pires, J. B., Siebeneichler, T. J., Kringel, D. H., et al. (2023). Encapsulation of anthocyanic extract of jambolan (Syzygium cumini (L.)) in zein sub-micron fibers produced by electrospinning. *Food Biophysics, 18*(1), 133–147.

Duan, M., Sun, J., Huang, Y., Jiang, H., Hu, Y., Pang, J., & Wu, C. (2023). Electrospun gelatin/chitosan nanofibers containing curcumin for multifunctional food packaging. *Food Science and Human Wellness, 12*(2), 614–621. https://doi.org/10.1016/J.FSHW.2022.07.064

Duan, M., Yu, S., Sun, J., Jiang, H., Zhao, J., Tong, C., et al. (2021). Development and characterization of electrospun nanofibers based on pullulan/chitin nanofibers containing curcumin and anthocyanins for active-intelligent food packaging. *International Journal of Biological Macromolecules, 187*, 332–340. https://doi.org/10.1016/j.ijbiomac.2021.07.140

Dumitriu, R. P., Stoleru, E., Mitchell, G. R., Vasile, C., & Brebu, M. (2021). Bioactive electrospun fibers of poly (ε-caprolactone) incorporating α-tocopherol for food packaging applications. *Molecules, 26*(18), 5498.

Ebrahimi, V., Mohammadi Nafchi, A., Bolandi, M., & Baghaei, H. (2022). Fabrication and characterization of a pH-sensitive indicator film by purple basil leaves extract to monitor the freshness of chicken fillets. *Food Packaging and Shelf Life, 34*, 100946. https://doi.org/10.1016/J.FPSL.2022.100946

Erez, E., & Bayramoglu, B. (2024). Evaluation of the extracts of purple basil (Ocimum basilicum L.) as natural pH-indicator dyes anticipated to be utilised in intelligent food packaging—an optimisation study. *Coloration Technology, 140*(6), 937–951. https://doi.org/10.1111/cote.12754

Forghani, S., Almasi, H., & Moradi, M. (2021). Electrospun nanofibers as food freshness and time-temperature indicators: A new approach in food intelligent packaging. *Innovative Food Science and Emerging Technologies, 73*(June), 102804. https://doi.org/10.1016/j.ifset.2021.102804

Freitas, P. A. V., Silva, R. R. A., de Oliveira, T. V., Soares, R. R. A., Junior, N. S., Moraes, A. R. F., et al. (2020). Development and characterization of intelligent cellulose acetate-based films using red cabbage extract for visual detection of volatile bases. *Lwt, 132*, 109780.

Gościniak, A., Rosiak, N., Szymanowska, D., Miklaszewski, A., & Cielecka-Piontek, J. (2024). Prebiotic systems containing anthocyanin-rich pomegranate flower extracts with antioxidant and antidiabetic effects. *Pharmaceutics, 16*(4), 526.

Goudarzi, J., Moshtaghi, H., & Shahbazi, Y. (2023). Kappa-carrageenan-poly(vinyl alcohol) electrospun fiber mats encapsulated with Prunus domestica anthocyanins and epigallocatechin gallate to monitor the freshness and enhance the shelf-life quality of minced beef meat. *Food Packaging and Shelf Life, 35*, 101017. https://doi.org/10.1016/J.FPSL.2022.101017

Guclu, N., DuzyerGebizli, S., & Orhan, M. (2023). Development of polycaprolactone-based electrospun pH-sensitive sensors as instant colorimetric indicators for food packaging. *Coloration Technology, 139*(5), 527–543. https://doi.org/10.1111/cote.12701

Haider, A., Haider, S., & Kang, I. K. (2018). A comprehensive review summarizing the effect of electrospinning parameters and potential applications of nanofibers in biomedical and biotechnology. *Arabian Journal of Chemistry, 11*(8), 1165–1188. https://doi.org/10.1016/j.arabjc.2015.11.015

He, H., Song, Y., Li, M., Zhang, H., Li, J., Huang, H., & Li, Y. (2023). A novel anthocyanin electrospun film by caffeic acid co-pigmentation for real-time fish freshness monitoring. *Analytical Methods, 15*(2), 228–239.

Hirano, N., Kusuhara, H., Sueyoshi, Y., Teramura, T., Murthy, A., Asamura, S., et al. (2021). Ethanol treatment of nanoPGA/PCL composite scaffolds enhances human chondrocyte development in the cellular microenvironment of tissue-engineered auricle constructs. *PLoS ONE, 16*(7), e0253149.

Houška, M., Silva, F. V. M., Evelyn, Buckow, R., Terefe, N. S., & Tonello, C. (2022). High pressure processing applications in plant foods. *Foods, 11*(2), 223. https://doi.org/10.3390/FOODS11020223

Hu, G., Li, J., Wang, Z., Yang, W., & Hu, Y. (2024). PCL/yam polysaccharide nanofibrous membranes loaded with self-assembled HP-β-CD/ECG inclusion complexes for food packaging. *Food Chemistry, 438*, 138031. https://doi.org/10.1016/J.FOODCHEM.2023.138031

Huang, K., Wang, Y., Xu, Z., Zou, Z., Tang, Q., Li, H., & Peng, D. (2024). Novel intelligent packaging films based on starch/PVA with Cu-ICA nanocrystal as functional compatibilizer for monitoring food freshness. *International Journal of Biological Macromolecules, 271*, 132373. https://doi.org/10.1016/J.IJBIOMAC.2024.132373

Jang, J. H., Kang, H. J., Adedeji, O. E., Kim, G. Y., Lee, J. K., Kim, D. H., & Jung, Y. H. (2023). Development of a pH indicator for monitoring the freshness of minced pork using a cellulose nanofiber. *Food Chemistry, 403*, 134366.

Jovanska, L., Chiu, C., Yeh, Y., & Chiang, W. (2022). Development of a PCL-PEO double network colorimetric pH sensor using electrospun fibers containing Hibiscus rosa sinensis extract and silver nanoparticles for food monitoring. *Food Chemistry, 368*(2021), 130813. https://doi.org/10.1016/j.foodchem.2021.130813

Kandi, R., Pandey, P. M., Majood, M., & Mohanty, S. (2021). Fabrication and characterization of customized tubular scaffolds for tracheal tissue engineering by using solvent based 3D printing on predefined template. *Rapid Prototyping Journal, 27*(2), 421–428.

Kang, S., Wang, H., Xia, L., Chen, M., Li, L., Cheng, J., et al. (2020). Colorimetric film based on polyvinyl alcohol/okra mucilage polysaccharide incorporated with rose anthocyanins for shrimp freshness monitoring. *Carbohydrate Polymers, 229*(July 2019), 115402. https://doi.org/10.1016/j.carbpol.2019.115402

Kaur, S., Sundarrajan, S., Rana, D., Matsuura, T., & Ramakrishna, S. (2012). Influence of electrospun fiber size on the separation efficiency of thin film nanofiltration composite membrane. *Journal of Membrane Science, 392*, 101–111.

Kopeć, K., Wojasiński, M., & Ciach, T. (2020). Superhydrophilic polyurethane/polydopamine nanofibrous materials enhancing cell adhesion for application in tissue engineering. *International Journal of Molecular Sciences, 21*(18), 6798.

Kotcharat, P., Chuysinuan, P., Thanyacharoen, T., Techasakul, S., & Ummartyotin, S. (2021). Development of bacterial cellulose and polycaprolactone (PCL) based composite for medical material. *Sustainable Chemistry and Pharmacy, 20*, 100404.

Li, N., Qin, H., Tang, Q., Peng, D., Luo, X., Li, H., & Zou, Z. (2024). Development and application of intelligent packaging films based on carboxymethyl starch/PVA with Cu-LTE nanocrystal as functional compatibilizer. *Food Packaging and Shelf Life, 43*, 101306. https://doi.org/10.1016/J.FPSL.2024.101306

Li, W., Sun, W., Jia, L., Dong, Y., Wu, L., Saldaña, M. D. A., & Sun, W. (2022). Poly-l-lactic acid (PLLA)/anthocyanin nanofiber color indicator film for headspace detection of low-level bacterial concentration. *International Journal of Biological Macromolecules, 215*, 123–131. https://doi.org/10.1016/J.IJBIOMAC.2022.06.034

Liu, L., Zhang, J., Zou, X., Arslan, M., Shi, J., Zhai, X., et al. (2022). A high-stable and sensitive colorimetric nanofiber sensor based on PCL incorporating anthocyanins for shrimp freshness. *Food Chemistry, 377*(July 2021), 131909. https://doi.org/10.1016/j.foodchem.2021.131909

Liu, X., Song, X., Gou, D., Li, H., Jiang, L., Yuan, M., & Yuan, M. (2023). A polylactide based multifunctional hydrophobic film for tracking evaluation and maintaining beef freshness by an electrospinning technique. *Food Chemistry, 428*, 136784. https://doi.org/10.1016/J.FOODCHEM.2023.136784

Luiza, A., Terra, M., Botelho, J., Alberto, J., Costa, V., Greque, M., & Morais, D. (2021). Development of time-pH indicator nanofibers from natural pigments : An emerging processing technology to monitor the quality of foods. *LWT, 142*(January), 111020. https://doi.org/10.1016/j.lwt.2021.111020

Lv, H., Wang, C., He, D., Zhao, H., Zhao, M., Xu, E., et al. (2024). Intelligent food tag: A starch-anthocyanin-based pH-sensitive electrospun nanofiber mat for real-time food freshness monitoring. *International Journal of Biological Macromolecules, 256*, 128384. https://doi.org/10.1016/j.ijbiomac.2023.128384

Mercante, L. A., Scagion, V. P., Migliorini, F. L., Mattoso, L. H. C., & Correa, D. S. (2017). Electrospinning-based (bio)sensors for food and agricultural applications: A review. *TrAC - Trends in Analytical Chemistry, 91*, 91–103. https://doi.org/10.1016/j.trac.2017.04.004

Mokrzycki, W. S., & Tatol, M. (2011). Colour differenceΔ EA survey. *Mach. Graph. vis, 20*(4), 383–411.

Moreira, J. B., Lim, L. T., da Rosa Zavareze, E., Dias, A. R. G., Costa, J. A. V., & de Morais, M. G. (2019). Antioxidant ultrafine fibers developed with microalga compounds using a free surface electrospinning. *Food Hydrocolloids, 93*, 131–136. https://doi.org/10.1016/j.foodhyd.2019.02.015

Moreira, J. B., Terra, A. L. M., Costa, J. A. V., & de Morais, M. G. (2018). Development of pH indicator from PLA/PEO ultrafine fibers containing pigment of microalgae origin. *International Journal of Biological Macromolecules, 118*, 1855–1862. https://doi.org/10.1016/J.IJBIOMAC.2018.07.028

Musso, Y. S., Salgado, P. R., & Mauri, A. N. (2017). Smart edible films based on gelatin and curcumin. *Food Hydrocolloids, 66*, 8–15. https://doi.org/10.1016/j.foodhyd.2016.11.007

Nur, F., & Parın, U. (2022). Spirulina biomass-loaded thermoplastic polyurethane / polycaprolacton (TPU/PCL) nanofibrous mats : Fabrication, characterization, and antibacterial activity as potential wound healing, *202104148*, 1–8. https://doi.org/10.1002/slct.202104148

Phippen, W. B., & Simon, J. E. (1998). Anthocyanins in basil (Ocimum basilicum L.). *Journal of Agricultural and Food Chemistry, 46*(5), 1734–1738. https://doi.org/10.1021/jf970887r

Prietto, L., Mirapalhete, T. C., Pinto, V. Z., Hoffmann, J. F., Vanier, N. L., Lim, L. T., et al. (2017). pH-sensitive films containing anthocyanins extracted from black bean seed coat and red cabbage. *LWT - Food Science and Technology, 80*, 492–500. https://doi.org/10.1016/j.lwt.2017.03.006

Prietto, L., Pinto, V. Z., El Halal, S. L. M., de Morais, M. G., Costa, J. A. V., Lim, L., et al. (2018). Ultrafine fibers of zein and anthocyanins as natural pH indicator. *Journal of the Science of Food and Agriculture, 98*(7), 2735–2741.

Rahma, A., Munir, M. M., Prasetyo, A., Suendo, V., & Rachmawati, H. (2016). Intermolecular interactions and the release pattern of electrospun curcumin-polyvinyl (pyrrolidone) fiber. *Biological and Pharmaceutical Bulletin, 39*(2), 163–173.

Sarkar, R., Dutta, A., Patra, A., & Saha, S. (2021). Bio-inspired biopolymeric coacervation for entrapment and targeted release of anthocyanin. *Cellulose, 28*, 377–388.

Schoolaert, E., Steyaert, I., Vancoillie, G., Geltmeyer, J., Lava, K., Hoogenboom, R., & De Clerck, K. (2016). Blend electrospinning of dye-functionalized chitosan and poly (ε-caprolactone): Towards biocompatible pH-sensors. *Journal of Materials Chemistry B, 4*(26), 4507–4516.

Shao, L., Chen, S., Wang, H., Zhang, J., Xu, X., & Wang, H. (2021). Advances in understanding the predominance, phenotypes, and mechanisms of bacteria related to meat spoilage. *Trends in Food Science & Technology, 118*, 822–832.

Shavisi, N., & Shahbazi, Y. (2022). Chitosan-gum Arabic nanofiber mats encapsulated with pH-sensitive Rosa damascena anthocyanins for freshness monitoring of chicken fillets. *Food Packaging and Shelf Life, 32*(December 2021), 100827. https://doi.org/10.1016/j.fpsl.2022.100827

Shi, C., Zhou, A., Fang, D., Lu, T., Wang, J., Song, Y., et al. (2022). Oregano essential oil/β-cyclodextrin inclusion compound polylactic acid/polycaprolactone electrospun nanofibers for active food packaging. *Chemical Engineering Journal, 445*, 136746.

Shi, S., Xu, X., Feng, J., Ren, Y., Bai, X., & Xia, X. (2023). Preparation of NH3- and H2S-sensitive intelligent pH indicator film from sodium alginate/black soybean seed coat anthocyanins and its use in monitoring meat freshness. *Food Packaging and Shelf Life, 35*, 100994. https://doi.org/10.1016/j.fpsl.2022.100994

Singh, S., Gaikwad, K. K., & Lee, Y. S. (2018). Anthocyanin – A natural dye for smart food packaging systems. *Korean Journal of Packaging Science and Technology, 24*(3), 167–180. https://doi.org/10.20909/kopast.2018.24.3.167

Solechan, S., Suprihanto, A., Widyanto, S. A., Triyono, J., Fitriyana, D. F., Siregar, J. P., & Cionita, T. (2022). Investigating the effect of PCL concentrations on the characterization of PLA polymeric blends for biomaterial applications. *Materials, 15*(20), 7396.

Sun, W., Liu, Y., Jia, L., Saldaña, M. D. A., Dong, T., Jin, Y., & Sun, W. (2021). A smart nanofibre sensor based on anthocyanin/poly-l-lactic acid for mutton freshness monitoring. *International Journal of Food Science & Technology, 56*(1), 342–351. https://doi.org/10.1111/ijfs.14648

Szewczyk, P. K., Ura, D. P., Metwally, S., Knapczyk-Korczak, J., Gajek, M., Marzec, M. M., et al. (2018). Roughness and fiber fraction dominated wetting of electrospun fiber-based porous meshes. *Polymers, 11*(1), 34.

Topuz, F., & Uyar, T. (2020). Antioxidant, antibacterial and antifungal electrospun nanofibers for food packaging applications. *Food Research International, 130*(August 2019), 108927. https://doi.org/10.1016/j.foodres.2019.108927

Van der Schueren, L., Mollet, T., Ceylan, Ö., & De Clerck, K. (2010). The development of polyamide 6.6 nanofibres with a pH-sensitive function by electrospinning. *European Polymer Journal, 46*(12), 2229–2239. https://doi.org/10.1016/j.eurpolymj.2010.09.016

Varesano, A., Carletto, R. A., & Mazzuchetti, G. (2009). Experimental investigations on the multi-jet electrospinning process. *Journal of Materials Processing Technology, 209*(11), 5178–5185.

Wen, X., Xiong, J., Lei, S., Wang, L., & Qin, X. (2022). Diameter refinement of electrospun nanofibers: From mechanism, strategies to applications. *Advanced Fiber Materials, 4*(2), 145–161. https://doi.org/10.1007/s42765-021-00113-8

Wongsasulak, S., Patapeejumruswong, M., Weiss, J., Supaphol, P., & Yoovidhya, T. (2010). Electrospinning of food-grade nanofibers from cellulose acetate and egg albumen blends. *Journal of Food Engineering, 98*(3), 370–376. https://doi.org/10.1016/j.jfoodeng.2010.01.014

Xu, R., Xia, L., Tang, Q., Tang, F., Pang, S., Li, H., & Zou, Z. (2024). High-performance carboxymethyl starch/PVA based intelligent packaging films engineered with Cu-Trp nanocrystal as functional compatibilizer. *Food Chemistry, 454*, 139696. https://doi.org/10.1016/J.FOODCHEM.2024.139696

Yildiz, E., Sumnu, G., & Kahyaoglu, L. N. (2021). International Journal of Biological Macromolecules Monitoring freshness of chicken breast by using natural halochromic curcumin loaded chitosan / PEO nano fi bers as an intelligent package. *International Journal of Biological Macromolecules, 170*, 437–446. https://doi.org/10.1016/j.ijbiomac.2020.12.160

Yuan, Y., and Lee, T. R. (2013). Contact angle and wetting properties. In *Surface science techniques* (pp. 3–34). Springer.

Zhai, X., Li, Z., Zhang, J., Shi, J., Zou, X., Huang, X., et al. (2018). Natural biomaterial-based edible and pH-sensitive films combined with electrochemical writing for intelligent food packaging. *Journal of Agricultural and Food Chemistry, 66*(48), 12836–12846. https://doi.org/10.1021/acs.jafc.8b04932

Zhang, C., Li, Y., Wang, W., Zhan, N., Xiao, N., Wang, S., et al. (2011). A novel two-nozzle electrospinning process for preparing microfiber reinforced pH-sensitive nano-membrane with enhanced mechanical property. *European Polymer Journal, 47*(12), 2228–2233. https://doi.org/10.1016/j.eurpolymj.2011.09.015

Zhang, J., Huang, X., Zhang, J., Liu, L., Shi, J., Muhammad, A., et al. (2022). Development of nanofiber indicator with high sensitivity for pork preservation and freshness monitoring. *Food Chemistry, 381*, 132224. https://doi.org/10.1016/J.FOODCHEM.2022.132224

Zou, Y., Sun, Y., Shi, W., Wan, B., & Zhang, H. (2023). Dual-functional shikonin-loaded quaternized chitosan/polycaprolactone nanofibrous film with pH-sensing for active and intelligent food packaging. *Food Chemistry, 399*, 133962. https://doi.org/10.1016/j.foodchem.2022.133962

Zou, Y., Chen, S., Dou, H., Zhu, W., Zhao, D., Wang, Y., et al. (2024). Development of a colorimetric nanofibrous film sensor based on polycaprolactone (PCL) incorporated with alizarin for tracking shrimp freshness. *Food Packaging and Shelf Life, 42*, 101249. https://doi.org/10.1016/j.fpsl.2024.101249

Publisher's Note Springer Nature remains neutral with regard to jurisdictional claims in published maps and institutional affiliations.